Polymer−Surfactant Vesicular Complexes in Aqueous Medium

Antonios Kelarakis,*,† Valeria Castelletto,‡ Marta J. Krysmann,‡ Vasiliki Havredaki,† Kyriakos Viras,† and Ian W. Hamley*,‡

Physical Chemistry Laboratory, Department of Chemistry, National and Kapodistrian University of Athens, Panepistimiopolis, 157 71 Athens, Greece, and School of Chemistry, The University of Reading, P.O. Box 224, Whiteknights, Reading RG6 6AD, UK

Received November 29, 2007. In Final Form: January 15, 2008

The introduction of ionic single-tailed surfactants to aqueous solutions of $EO_{18}BO_{10}$ [EO = poly(ethylene oxide), BO = poly(1,2-butylene oxide), subscripts denote the number of repeating units] leads to the formation of vesicles, as probed by laser scanning confocal microscopy. Dynamic light scattering showed that the dimensions of these aggregates at early stages of development do not depend on the sign of the surfactant head group charge. Small-angle X-ray scattering (SAXS) analysis indicated the coexistence of smaller micelles of different sizes and varying polymer content in solution. In strong contrast to the dramatic increase of size of dispersed particles induced by surfactants in dilute solution, the *d*-spacing of corresponding mesophases reduces monotonically upon increasing surfactant loading. This effect points to the suppression of vesicles as a consequence of increasing ionic strength in concentrated solutions. Maximum enhancements of storage modulus and thermal stability of hybrid gels take place at different compositions, indicating a delicate balance between the number and size of polymer-poor aggregates (population increases with surfactant loading) and the number and size of polymer−surfactant complexes (number and size decrease in high surfactant concentrations).

1. Introduction

The association properties of aqueous solutions of copolymers comprising poly(ethylene oxide) coupled with hydrophobic blocks of poly(propylene oxide) or poly(1,2-butylene oxide) (notated as EO/BO and EO/PO, respectively, hereafter) have received much interest in recent years and several extensive reviews summarize the progress achieved in this field.[1−4] The fundamental physicochemical parameters of micellization have been interpreted with respect to block architecture, block length, and chemical nature of the hydrophobic units. Considerably less attention has been given to the study of the interactions between macromolecular amphiphiles of this type and ionic surface-active agents. Nevertheless, it has been well-established that in the presence of some typical anionic or cationic surfactants, the aggregation properties of EO/PO copolymers are significantly altered.[5] The polyelectrolyte characteristics of these complexes, originating from their hybrid nature, make them promising candidates for a wide range of possible applications, such as templates for the development of nanoscale materials, drugs, coatings, pharmaceutical, and petroleum and detergent formulations. In the field of nanotechnology, inclusion of ionic surfactants in the polymeric micellar core can essentially reverse their inherent nonpolar characteristics, facilitating their application as nanoreactors for engineering of metal colloids in nano- and subnanoscales.[6]

An understanding of the physical interactions between EO/PO and surfactants can be traced back to the well-studied absorption of charged hydrocarbon tails to poly(propylene oxide) sequences.[7,8] The spontaneous binding between anionic single-tailed surfactants and EO/PO copolymers was first manifested on the basis of the lower critical aggregation concentration (cac) of SDS in EO/PO-enriched aqueous environment compared to the critical micelle concentration (cmc) of SDS in water.[9] From the copolymer point of view, an early work[10] showed that SDS addition favors the suppression of EO/PO micelles, an observation that was further explored in a number of later reports. Detailed investigations on the binding mechanism of $EO_{97}PO_{69}EO_{97}$ (Pluronic F127) revealed four distinct steps of interaction: polymer micellization induced by SDS,[11] formation of SDS−polymer complexes, collapse of complexes, and complete inhibition of micellar growth.[12−15]

Besides EO/PO copolymers, studies of poly(ethylene oxide)-based copolymer−surfactants interactions have been extended to other systems having polystyrene (PS),[6,16−20] polystyrene oxide

* Corresponding authors. E-mail: akelar@cc.uoa.gr (A.K.), i.w.hamley@reading.ac.uk (I.W.H.).

† National and Kapodistrian University of Athens.

‡ The University of Reading.

(1) Booth, C.; Attwood, D. *Macromol. Rapid Commun.* **2000**, *21*, 501.
(2) Booth, C.; Attwood, D.; Price, C. *Phys. Chem. Chem. Phys.* **2006**, *8*, 3612.
(3) *Nonionic Surfactants, Poly(oxyalkylene) Block Copolymers*; Nace, V. M., Ed.; Surfactant Science Series; Marcel Dekker, New York, 1996; vol. 60.
(4) Hamley, I. W. *The Physics of Block Copolymers*; Oxford University Press: New York, 1998
(5) Sastry, N. V.; Hoffmann, H. *Colloids Surf. A* **2004**, *250*, 247 and references therein.
(6) Bronstein, L. M.; Chernyshov, D. M.; Timofeeva, G. I.; Dubrovina, L. V.; Valetsky, P. M.; Obolonkova, E. S.; Khokhlov, A. R. *Langmuir* **2000**, *16*, 3626.
(7) Brackman, J. C.; Engberts, J. B. F. N. *Langmuir* **1991**, *7*, 2097
(8) Brackman, J. C.; Engberts, J. B. F. N. *Langmuir* **1992**, *8*, 424
(9) Cabane, B.; Duplesix, *J. Phys. (Paris)* **1982**, 43, 1529
(10) Almgren, M.; van Stam, J.; Lindblad, C.; Li, P.; Stilbs, P.; Bahadur, P. *J. Phys. Chem.* **1991**, *95*, 5677.
(11) Li, Y.; Xu. R.; Couderc, S.; Bloor, D. M.; Wyn-Jones, E.; Holzwarth, J. F. *Langmuir* **2001**, *17*, 183.
(12) Hecht, E.; Hoffmann, H. *Langmuir* **1994**, *10*, 86.
(13) Hecht, E.; Mortensen, K.; Gradzielski, M.; Hoffmann, H. *J. Phys. Chem.* **1995**, *99*, 4866.
(14) Hecht, E.; Hoffmann, H. *Colloids Surf.* **1995**, *96*, 181.
(15) Ghoreishi, S. M.; Fox, G. A.; Bloor, D. M.; Holzwarth, J. F.; Wyn-Jones, E. *Langmuir* **1999**, *15*, 5474.
(16) Nakamura, K.; Endo, R.; Masatani, T. *J. Polym. Sci. Polym. Phys. Ed.* **1977**, *15*, 2087.
(17) Bahadur, P.; Sastry, N. V.; Rao, Y. K.; Riess, G. *Colloids Surf.* **1988**, *29*, 343.
(18) Contractor, K.; Patel, C.; Bahadur, P. *J. Macromol. Sci. Pure Appl. Chem.* **1997**, *A34*, 2497.
(19) Bronstein, L. M.; Chernyshov, D. M.; Timofeeva, G. I.; Dubrovina, L. V.; Valetsky, P. M.; Khokhlov, A. R. *J. Colloid Interface Sci.* **2000**, *230*, 140.
(20) Bronstein, L. M.; Chernyshov, D. M.; Vorontsov, E.; Timofeeva, G. I.; Dubrovina, L. V.; Valetsky, P. M.; Kazakov, S.; Khokhlov, A. R. *J. Phys. Chem.* **2001**, *105*, 9077.

10.1021/la703745z CCC: $40.75
Published on Web 03/04/2008

(PSO),[21,22] and polybutadiene (PB)[23−25] as the hydrophobic block. In this contribution, we focus on the interaction mechanism of nonionic copolymer $EO_{18}BO_{10}$ with anionic and cationic single-tailed surfactants (namely, sodium dodecyl sulfate, sodium decyl sulfate, and hexadecyltrimethylammonium bromide). The particular interest in this copolymer[26−35] arises from its low hydrophilic/hydrophobic unit ratio. This structural characteristic allows the elongation of spherical micelles toward wormlike aggregates under certain conditions.[35] In analogy, aqueous mesophases with face-centered cubic (fcc), hexagonal, or lamellar morphology can be obtained from concentrated solutions, completing a rich phase diagram. The aim of this report is to investigate the structures and the properties of $EO_{18}BO_{10}$−surfactant complexes in dilute, semidilute, and concentrated aqueous solutions and explore the interaction mechanism in hybrid systems of this kind.

2. Experimental Section

2.1. Materials. Sodium dodecyl sulfate (SDS), sodium decyl sulfate (SDecS), hexadecyltrimethylammonium bromide or cetyltrimethylammonium bromide (CTAB), all with stated purity >99%, were purchased from Acros Organics and were dried before use. $EO_{18}BO_{10}$ (also denoted $EO_{18}BO_9$ [26,33,34] and EB 18−9[27] in other studies) was obtained from Dow Chemical Co. (code BM45-1600). The sample was characterized by gel permeation chromatography (GPC) to obtain the ratio of mass average to number average molar mass $M_w/M_n = 1.04$ and ^{13}C NMR to give $M_n = 1510$ g/mol.

Copolymer dilute solutions in distilled water were used as stock solutions for the preparation of surfactant−copolymer samples. For concentrated gels, both surfactants and polymer were inserted in small vials, mixed with distilled water, and sheared for several hours until complete dissolution.

2.2. Methods. *Laser Scanning Confocal Microscopy (LSCM).* Imaging was performed on a Leica TCS SP2 confocal system mounted on a Leica DM-IRE2 inverted microscope, using a 63× glycerol emulsion objective with a 1.3 NA numerical aperture. The sample was imaged in solution in the presence of the dye rhodamine B (dissolved in double-distilled deionized water at a concentration of 0.5 g/100 mL). The excitation wavelength generated by a green HeNe laser was 543 nm, while the emission detection was in the range of 557−671 nm.

Dynamic Light Scattering (DLS). Dynamic light scattering (DLS) measurements were carried out on well-filtered solutions by means of an ALV/CGS-3 compact goniometer system with ALV/LSE-5003 correlator using vertically polarized incident light of wavelength $\lambda = 632.8$ nm. Measurements were performed at an angle $\theta = 90°$ to the incident beam and data were collected three times for 30 s. The intensity correlation functions were analyzed by the constrained regularized CONTIN method[36] to obtain distributions of decay rates (Γ) and hence distributions of apparent mutual diffusion coefficient $D_{app} = \Gamma/q^2$ [$q = (4\pi n/\lambda)\sin(\theta/2)$, where n is the refractive index of the solvent] and ultimately of the apparent hydrodynamic radius of the particle via the Stokes−Einstein equation

$$r_{h,app} = kT/(6\pi\eta D_{app}) \quad (1)$$

where k is the Boltzmann constant and η is the viscosity of the solvent at temperature T.

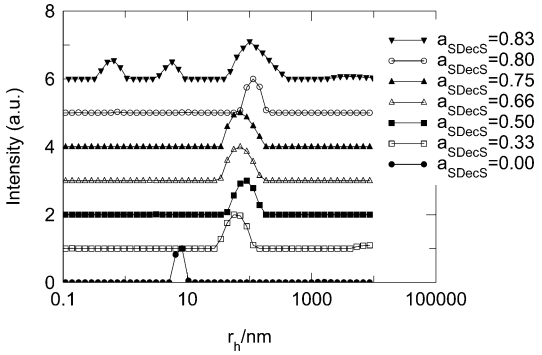

Figure 1. Normalized intensity fraction distributions of apparent hydrodynamic radius (r_h) for an aqueous solution of $EO_{18}BO_{10}$−SDecS complexes with various molar fraction of the surfactant (copolymer concentration was kept constant 1 wt %, $T = 25$ °C, samples aged for 2 weeks).

Small-Angle X-ray Scattering (SAXS). SAXS experiments were performed on beamline 2.1, Synchrotron Radiation Source, Daresbury, U.K. The wavelength of synchrotron radiation was $\lambda = 1.5$ Å and the sample-to-detector distance was 3 m. Samples were mounted between mica windows in a homemade liquid cell with water-bath temperature control. Two-dimensional SAXS patterns were collected using a RAPID area detector. All patterns were corrected for the incident beam fluctuations as well as air and instrument scattering. The SAXS q scale ($q = 4\pi \sin\theta/\lambda$, where 2θ is the scattering angle) was calibrated by using collagen rat tendon standards. 2-D SAXS patterns were converted to 1-D profiles using BSL software.

Rheology. Rheological properties were determined using a controlled stress TA Instruments AR-2000 rheometer (TA Instruments). A cone and plate geometry (cone diameter 20 mm, angle 1°) was used for all samples. Temperature scans were performed within the range 15−60 °C, with the instrument in oscillatory mode at an angular frequency of 10 rad/s. The samples were heated at 1 °C/min. Preliminary strain sweeps were performed for each sample in order to define the linear viscoelastic region, thus ensuring that moduli were independent of strain.

3. Results and Discussion

3.1. Complexation in Solution. Intensity fraction distributions of the apparent hydrodynamic radius (r_h) of aqueous solutions of 1 wt % $EO_{18}BO_{10}$ solution in the presence of various mole fractions of SDecS (a_{SDecS}) ($a_{surfactant}$ = moles of ionic surfactant/moles of polymer+surfactant) are illustrated in Figure 1. It can be seen that introduction of SDecS to aqueous solutions of $EO_{18}BO_{10}$ leads to the formation of large particles with $r_h \approx 100$ nm, while pure $EO_{18}BO_{10}$ micelles have $r_h \approx 7$ nm. These large complexes are stable up to $a_{SDecS} = 0.80$ but start destabilizing upon further addition of SDecS, indicating a saturation point of five SDecS molecules per single polymer chain. Polymer−surfactants complexes with molar fraction approximately 1−5 have been also reported for the mixture of SDS with EO/PO[9] and EO/PS[19] block copolymers.

(21) Castro, E.; Taboada, P.; Mosquera, V. *J. Phys. Chem. B* **2005**, *109*, 5593.
(22) Taboada, P.; Castro, E.; Mosquera, V. *J. Phys. Chem. B* **2005**, *109*, 23760.
(23) Zheng, Y.; Davis, H. T. *Langmuir* **2000**, *16*, 6453.
(24) Pispas, S.; Hadjichristidis, N. *Langmuir* **2003**, *19*, 48.
(25) Egger, H.; Nordskog, A.; Lang, P.; Brandt, A. *Macromol. Symp.* **2000**, *162*, 291.
(26) Yu, G. E.; Yang, Y. W.; Yang, Z.; Attwood, D.; Booth, C.; Nace, V. M. *Langmuir* **1996**, *12*, 3404.
(27) Nace, V. M. *J. Am. Oil Chem. Soc.* **1996**, *73*, 1.
(28) Alexandridis, P.; Olsson, U.; Lindman, B. *Langmuir* **1997**, *13*, 23.
(29) Pople, J. A.; Hamley, I. W.; Fairclough, J. P. A.; Ryan, A. J.; Booth, C. *Macromolecules* **1998**, *31*, 2952.
(30) Hamley, I. W.; Pederson, J. S.; Booth, C.; Nace, V. M. *Langmuir* **2001**, *17*, 6386.
(31) Kelarakis, A.; Mai, S. M.; Havredaki, V.; Nace, V. M.; Booth, C. *Phys. Chem. Chem. Phys.* **2001**, *3*, 4037.
(32) Kelarakis, A.; Havredaki, V.; Booth, C.; Nace, V. M. *Macromolecules* **2002**, *35*, 5591.
(33) Soni, S. S.; Sastry, N. V.; Patra, A. K.; Joshi, J. V.; Goyal, P. S. *J. Phys. Chem. B* **2002**, *106*, 13069.
(34) Norman, A. I.; Ho, D. L.; Karim, A.; Amis, E. J. *J. Colloid Interface. Sci.* **2005**, *205*, 155.
(35) Harris, J. K.; Rose, G. D.; Bruening, M. L. *Langmuir* **2002**, *18*, 5337.
(36) Provencher, S. W. *Makromol. Chem.* **1979**, *180*, 201.

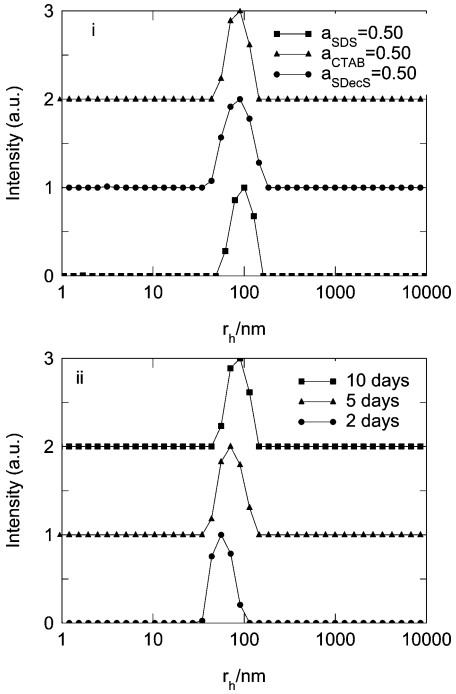

Figure 2. Normalized intensity fraction distributions of apparent hydrodynamic radius (r_h) ($T = 25$ °C) for aqueous solution of 1 wt % $EO_{18}BO_{10}$ in the presence of (i) 0.50 molar fraction of various surfactants (all samples aged for 2 weeks) and (ii) 0.5 molar fraction of CTAB at several equilibrium times.

It should be noted that large polymer−surfactant complexes of the same magnitude were observed upon addition of anionic SDS or cationic CTAB. This is evident in Figure 2i, which shows the r_h distribution of 1 wt % $EO_{18}BO_{10}$ aqueous solutions in the presence of SDS, SDecS, and CTAB, all of which have $a_{surfactant} = 0.50$. Therefore, the size of the polyelectrolyte complexes formed by $EO_{18}BO_{10}$ is not sensitive either to the anionic or cationic nature nor to the tail length of the added surfactant. It should be noted, however, that it is well-documented that many water-soluble polymers exhibit stronger tendency for binding with anionic rather than cationic surfactants.[37] On the other hand, several reports underline the lack of selectivity of PEO-based copolymers with respect to positive or negative charges of the head group of surfactants; for example, it was shown that both SDS and CTAB have the same efficiency in suppressing F127 micellization.[12] In the present study, it was found that the saturation point for both anionic surfactants is close to a polymer/surfactant molar ratio of 1/5, while a ratio of 1/4 was found for CTAB. The breakdown of complexes takes place at a lower surfactant loading in the case of cationic surfactants compared to anionic, much as reported in related studies.[17,38]

The kinetics of growth of these complexes is another point of interest. In all cases, the size of complexes gradually increased after initial mixing of the components during the first few days. An indicative example is demonstrated in Figure 2ii for $EO_{18}BO_{10}$−CTAB, $a_{CTAB} = 0.50$. Lower values of r_h in the first stages of complex growth were found for solutions with lower surfactant loading. Given that all possible interactions are physical in nature, these kinetic parameters underline the action of a multistep mechanism, possibly involving slow diffusive motions of the particles. Upon further aging over a period of 3 months, solutions became cloudy, indicating phase separation, much as expected for vesicular particles.

The size of aggregates remains essentially unaltered upon heating up to 60 °C, despite the fact that purely polymeric micelles undergo a sphere to rod transition within this temperature range, increasing dramatically their size.[30,34] As mentioned in the Introduction, the formation of wormlike micelles has been investigated in detail,[30−34] and the temperature-induced micellar elongation has been ascribed to the partial drainage of ethylene oxide corona due to weakening of H-bridges. The shrinkage of the hydrophilic block enables higher association numbers, and the geometrical transition takes place when the radius of the micellar core exceeds the fully stretched length of the hydrophobic block.[1,30,34,39]

In copolymer−surfactant aqueous solutions, the dispersed particles could in principle adopt a number of possible conformations: unimers of surfactants and copolymers, absorbed charged chains in the microdomains of the hydrophobic backbone of the polymer, and hybrid aggregates having a wide range of compositions varying from micelles with primarily polymeric content to single polymer chains surrounded by a definite number of surfactant molecules. An association model that had been originally developed for the F127−SDS system that assumes the existence of parallel equilibria between all possible configurations[13] seems to be applicable in several related mixtures where destabilization of micelles is the dominant effect. On the basis of this approach, mixed micelles progressively break down upon increasing ionic loading due to increased repulsive interactions between the charged groups included in the complex structure.

Although it was not possible to obtain SAXS data corresponding to the dimensional range of the large complexes, experiments were performed in an attempt to detect and characterize any possible coexisting structures with smaller dimensions, given that DLS plots are dominated by the strong signal of large aggregates.

The small-angle X-ray scattering intensity, $I(q)$, of an isotropic solution of spherical particles can be written as

$$I(q) = kP(q)\,S(q) \qquad (2)$$

where k is a normalization constant proportional to the number density of scatterers, $P(q)$ is the form factor, $S(q)$ is the structure factor, and q is the scattering vector. For widely separated systems, $S(q) \sim 1$ in eq 2, so $I(q)$ is proportional to the form factor $P(q)$.

To fit the SAXS data, we used an expression for $P(q)$ based on a homogeneous micellar core with attached Gaussian chains.[40] Data were fitted using SASfit software. The six fitting parameters are the micellar core radius, R; the association number, N; the radius of gyration of the chains in the corona, R_g; the displacement of the chains in the corona from the core surface, α; and the excess electron densities, β_x, of a blocks in the core (x = s) or in the corona (x = c).

Figure 3 shows the SAXS curves obtained for 2.5 wt % polymer and 2.5 wt % polymer−SDS, $a_{SDS} = 0.5$. The full line in Figure 3 corresponds to the fitting obtained according to the model described in the paragraph above. The deviations at very low q for the 2.5 wt % polymer sample are due to intermicellar interactions, not considered in the model. The parameters obtained from the fits are listed in Table 1. The SAXS data for 2.5 wt % polymer was fitted according to a single population of micelles, while the data for 2.5 wt % polymer−SDS, $a_{SDS} = 0.5$ was fitted according to two different populations of micelles characterized

(37) Moroi, Y.; Akisada, H.; Saito, M.; Matuura, R. *J. Colloid Interface Sci.* **1977**, *61*, 233.
(38) Cardaso da Silva, R.; Olofsson, G.; Schillen, K.; Loh, W. *J. Phys. Chem. B* **2002**, *106*, 4818.
(39) Mortensen, K.; Pedersen, J. S. *Macromolecules* **1993**, *26*, 4128.
(40) Pedersen, J. S.; Gerstenberg, M. C. *Macromolecules* **1996**, *29*, 1363.

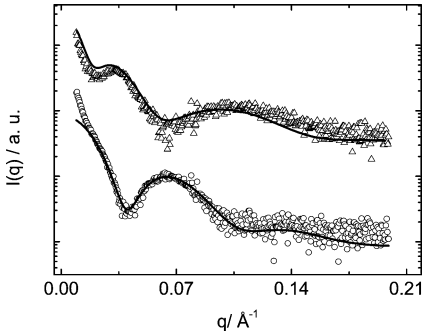

Figure 3. SAXS data for (○) 2.5 wt % polymer and (△) 2.5 wt % $EO_{18}BO_{10}$−SDS (a_{SDS} = 0.50) (samples aged for 2 weeks). The SAXS curves have been shifted in order to enable the data visualization. The full line corresponds to the fitting of the data as described by the text.

Table 1. Parameters Obtained from the Fitting of the SAXS Curves in Figure 4

sample	R/Å	R_g/Å	a	N	β_s/e Å^{-1}	β_c/e Å^{-1}
2.5 wt % $EO_{18}BO_{10}$	40	22	0.7	50	−0.00038	0.00012
2.5 wt % $EO_{18}BO_{10}$-SDS, a_{SDS} = 0.50						
population 1	70	52	0.7	50	−0.00069	0.0002
population 2	28	10	1	50	0.00038	0.00012

by R= 70 Å and 28 Å, respectively. No polydispersity effects were necessary to model any of the SAXS curves shown in Figure 3; this points to systems of relatively monodisperse micelles (a rough estimation could be that the polydispersity is lower than 30 wt %). This result leads, for the 2.5 wt % polymer−SDS (a_{SDS} = 0.5) sample, into two well-defined populations of micelles characterized by R = 70 Å and 28 Å, respectively, which do not correspond to a broad distribution with a two-component model.

The results in Table 1 show that, for the pure polymer solution, micelles with a total radius $R_T = R + (1 + \alpha)R_g$ = 78 Å are present in the solution, consistent with light-scattering data (Figure 1). However, the addition of SDS to the system leads to the formation of two populations of micelles with R_T = 48 and 158 Å. The SAXS data in this work have not been measured using an absolute scale (i.e., k in eq 2 has not been calculated). Consequently, β_s and β_c do not represent absolute values [since they are multiplicative constants in $P(q)$]. Nevertheless, it was found that the electron density of the smaller micelles in the polymer−SDS system is the same as the electron density of the pure polymer micelles, indicating that SDS is not incorporated to the micelles with R = 28 Å. In contrast, β_s and β_c for the bigger micelles in the ternary system are different from the electron density of the pure polymer micelles. This result indicates that SDS is included in particles with R = 70 Å; the presence of SDS modifies the β_s and β_c of the resulting polymer−surfactant complexes compared to the pure polymeric micelles. All in all, SANS analysis supports the shrinkage of the pure polymeric micelles induced by SDS and the formation of polymer−surfactant complexes with R_T = 158 Å.

While the most common pattern of EO-based copolymer−surfactant interaction is that of destabilized ethylene oxide/alkylene oxide (EO/AO) micelles, there is increasing evidence in the literature that the presence of ionic surfactants can induce additional effects. It has been shown that addition of cetylpyridinium chloride (CPC) to PSt−EO solutions can induce the formation of large aggregates,[6] and addition of SDS or DTAB in PB−PEO solution can cause the transformation of spherical micelles to large clusters or vesicles, the more so for polymers having lengthy hydrophobic units.[24] Large particles were also

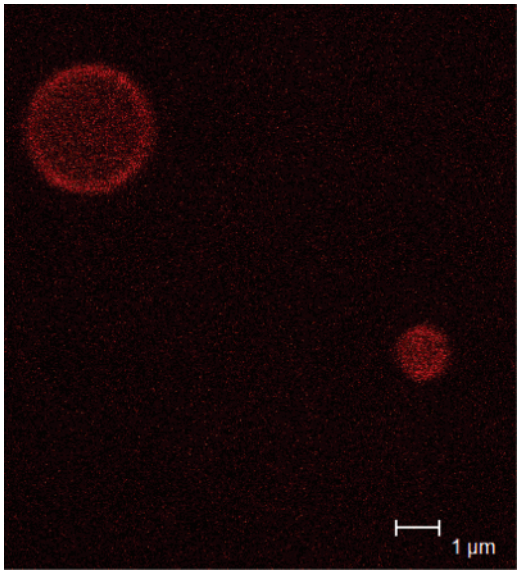

Figure 4. Laser confocal scanning micrograph of 2.5 wt % $EO_{18}BO_{10}$−SDS (a_{SDS} = 0.50) complexes in aqueous environment.

detected in PEO/PSO−SDS solutions,[22] while in another PEO/PSO−SDS system a nonmonotonic decrease of r_h upon increasing SDS loading was monitored.[21]

Although a multiequilibration status also holds for $EO_{18}BO_{10}$−surfactants, case specific thermodynamic parameters in this system favor the evolution of large complexes. Laser scanning confocal microscopy (LSCM) revealed the existence of vesicular structures having a wide distribution in size. A representative picture is given in Figure 4 for $EO_{18}BO_{10}$−SDS, a_{SDS} = 0.50 that was aged for 2 weeks. Therefore, the incorporation of charged surfactant tails to the micellar core can promote water penetration, giving rise to vesicle formation. The particles with radius in the range of 500−1000 nm observed from LCSM are part of a large distribution of sizes of vesicles formed in $EO_{18}BO_{10}$−surfactants solutions. Self-organization of amphiphiles toward the formation of vesicular structures has been viewed as an interplay between thermodynamic and kinetic contributions.[41,42] Several nonionic-surfactant-based vesicles have been studied,[43] including short-chain poly(ethylene oxide)-based copolymers[44] and EO/BO.[45,46] However, the micellar to vesicular transition in any EO-based copolymers induced solely by surfactant has not been reported so far.

In order to obtain insights into the structural characteristics of concentrated solutions discussed in the following paragraphs, we performed a brief DLS investigation on semidilute solutions of $EO_{18}BO_{10}$−SDS. In Figure 5 the intensity distributions of r_h of 10 and 15 wt % $EO_{18}BO_{10}$ (this is the maximum concentration of a $EO_{18}BO_{10}$−SDS solution that can be filtered according to our usual DLS protocol; see Experimental Section) in water are plotted together with corresponding data obtained in the presence of SDS. The progressive shrinkage of the pure copolymer micelles upon increasing concentration (Figures 1 and 4) indicates a certain degree of micelle compression due to increased interparticle interactions arising from excluded volume effects. The observed trimodal distribution for the hybrid semidilute solutions can be

(41) Lasic, D. D. *Nature* **1991**, *351*, 613.
(42) Discher, D. E.; Eisenberg, A. *Science* **2002**, *297*, 967.
(43) Uchegbu, I. F.; Vyas, S. P. *Int. J. Pharm.* **1998**, *172*, 33.
(44) Kickelbick, G.; Bauer, J.; Husing, N.; Andersson, M.; Palmqvist, A. *Langmuir* **2003**, *19*, 3198.
(45) Battaglia, G.; Ryan, A. J. *J. Am. Chem. Soc.* **2005**, *127*, 8757.
(46) Battaglia, G.; Ryan, A. J. *J. Phys. Chem. B* **2006**, *110*, 10272.

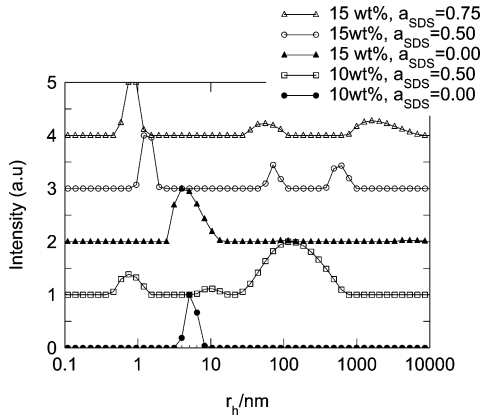

Figure 5. Normalized intensity fraction distributions of apparent hydrodynamic radius (r_h) ($T = 25$ °C) for aqueous solutions of 10 and 15 wt % of $EO_{18}BO_{10}$ and the corresponding $EO_{18}BO_{10}$−SDS complexes ($a_{SDS} = 0.50$) (samples aged for 2 weeks).

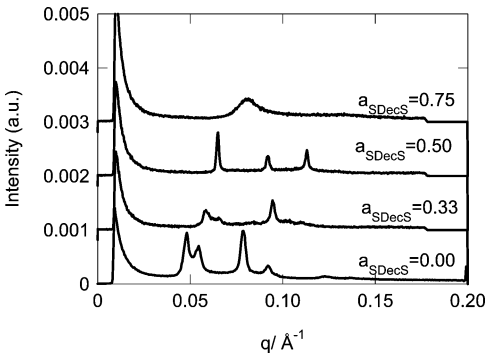

Figure 6. SAXS patterns of aqueous mesophases of $EO_{18}BO_{10}$−SDecS complexes (copolymer concentration was kept constant 24 wt %, $T = 25$ °C)

attributed to surfactant rich aggregates (low r_h), surfactant−polymer complexes (moderate r_h), and clusters of complexes (slow diffusive mode). We note here that the number of these large clusters is extremely small (lower than 0.1% based on DLS intensity signal) and thus we will hereafter consider solely the existence of the other two modes. All in all, the increased ionic strength in semidilute solutions dramatically modifies the nature of dispersed particles, favoring the formation of surfactant rich complexes, while a certain amount of aggregates with the same nature as those found in the dilute regime are still preserved.

3.2. Complexation in Aqueous Mesophases. SAXS patterns obtained for 24 wt % $EO_{18}BO_{10}$ having various loadings of SDecS are shown in Figure 6. On the basis of the location of the first maximum (q^*) in the scattering patterns, the relevant domain−domain distance d (calculated from the expression $d = 2\pi/q^*$) was found to reduce from 130.8 to 107 to 96 Å for $a_{SDecS} = 0.00$, 0.33, and 0.50, respectively. The scattering peaks of the SAXS profile correspond to fcc packing for $a_{SDecS} = 0.00$ and 0.33 and to body-centered cubic (bcc) packing for $a_{SDS} = 0.50$. For $a_{SDecS} = 0.75$, the presence of a broad peak suggests the formation of a disordered structure. Similar results were obtained for $EO_{18}BO_{10}$−SDS and $EO_{18}BO_{10}$−CTAB systems.

In other words, in contrast to the dramatic increase of the size of dispersed particles induced by surfactants in the dilute solution, the d-spacing of gels reduces monotonically upon increasing surfactant loading. This effect can be attributed to the stabilization of smaller aggregates at the expense of superaggregates within the gel phase. Moreover, the size and the population of the large polyelectrolyte complexes decrease upon increasing the amount

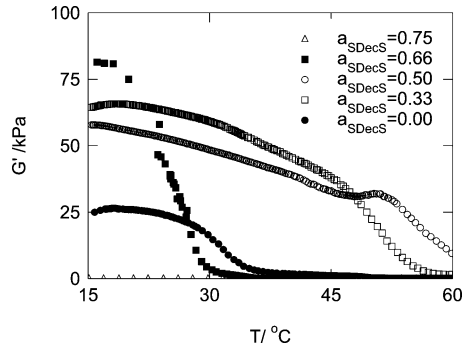

Figure 7. Temperature dependence of storage modulus (G') ($\omega =$ 10 rad/s, strain amplitude = 0.5%) for aqueous gels of $EO_{18}BO_{10}$−SDecS complexes (copolymer concentration was kept constant 24 wt %)

of added surfactant, as a direct consequence of the increased ionic strength, which suppresses the growth of large particles and promotes the development of small aggregates.

The delicate balance between the two main dispersed species is reflected in Figure 7, which shows the viscoelastic properties of gels having various degrees of ionic surfactant loading. A significant enhancement of storage modulus (G') was observed for several compositions of $EO_{18}BO_{10}$−surfactants systems, and at the same time, the temperature zone of gel stability was expanded. This behavior supports the presence of strong polymer−surfactant interactions even at highly concentrated gels. On the other hand, addition of $a_{SDecS} = 0.75$ ($a_{SDS} = 0.75$, $a_{CTAB} = 0.85$) resulted in complete melting of the gel. Studies on related systems showed that the decomposition of the gel phase was due to destabilization of micelles induced by surfactants.[13,47]

We note that at 25° C the highest G' was observed for $a_{SDecS} = 0.33$, while a lower value was found for $a_{SDecS} = 0.50$; e.g., the close-backed fcc structure exhibits stronger viscoelasticity compared to the bcc structure. At the same time, the maximum G' (at $T = 15$ °C) was found for $a_{SDecS} = 0.66$, whereas the maximum thermal stability (highest temperature where $G' > G''$) was found for $a_{SDecS} = 0.50$. The rheological behavior of these hybrid systems can be explained as follows. Addition of surfactant induces the presence of large aggregates and thus enhances viscoelasticity. Increasing surfactant loading results in an increasing population of small particles that can occupy the free space not occupied between two superaggregates, enhancing the viscoelasticity of the system. A further increase in surfactant loading increases the concentration of surfactant-rich complexes, on one hand, and destabilizes the superaggregates by decreasing both their size and their population, on the other hand. Compositions with maximum G' have the most compact packing (maximum space occupied), while compositions of maximum thermal stability have an optimum balance of polymeric content necessary to form a transient network and surfactant content to induce complexation.

Conclusions

We demonstrate here a unique case of EO-based copolymer−surfactant complexation that leads to vesicle structures, with dispersed particles having hydrodynamic radius in the range of few hundred nanometers. These structures develop in size with time, following a multiequilibrium status between several particles with various size and polymeric content. In strong contrast to the dramatic increase of size of dispersed particles induced by single-

(47) Ivanova, R.; Alexandridis, P.; Lindman, B. *Colloids Surf. A* **2001**, *183−185*, 41

tailed surfactants in dilute solution, the *d*-spacing of corresponding gels reduces monotonically upon increasing surfactant loading. This effect can be attributed to the stabilization of smaller aggregates at the expense of vesicular structures within the gel phase. Maximum enhancements of storage modulus and thermal stability of hybrid gels were observed at different mixture compositions, indicating a delicate balance between the number and size of polymer-poor aggregates (population increases with surfactant loading) and the number and size of polymer−surfactant complexes (number and size decrease at high surfactant concentrations).

Acknowledgment. A.K. was supported by the Greek Ministry of Development-General Secretariat of Research and Technology within the 04EP36 research project. The authors thank Mr. Stephen Pountney (School of Biological Sciences, The University of Reading) for assistance with LSCM.

LA703745Z